Article:
Bachollet, S.P., Volz, D., Fiser, B. et al. (2016) A Modular Class of Fluorescent Difluoroboranes: Synthesis, Structure, Optical Properties, Theoretical Calculations and Applications for Biological Imaging. Chemistry, 22 (35). pp. 12430-12438. ISSN: 0947-6539

https://doi.org/10.1002/chem.201601915

A Modular Class of Fluorescent Difluoroboranes: Synthesis, Structure, Optical Properties, Theoretical Calculations and Applications for Biological Imaging

Sylvestre P. J. T. Bachollet,[a, b] Daniel Volz,[c] Béla Fiser,[d] Stephan Münch,[b] Franziska Rönicke,[e] Jokin Carrillo,[a] Harry Adams,[a] Ute Schepers,[e] Enrique Gómez-Bengoa,[d] Stefan Bräse*[b] and Joseph P. A. Harrity*[a]

Abstract: Ten borylated bipyridines (BOBIPYs) have been synthesized and selected structural modifications have been made that allow useful structure-optical property relationships to be gathered. These systems have been further investigated using DFT calculations and spectroscopic measurements, showing blue to green fluorescence with quantum yields up to 41%. They allow full mapping of the structure to determine where selected functionalities can be implemented, to tune the optical properties or to incorporate linking groups. The best derivative was thus functionalised with an alkyne linker, which would enable further applications through click chemistry and in this optic, the stability of the fluorophores has been evaluated.

Introduction

Fluorescent molecules have been of particular interest recently, and they have found applications in numerous fields, such as materials sciences,[1] laser dyes,[2] fluorescent switches,[3] chemosensors,[4] photodynamic therapy[5] and biological imaging.[6] Organoboron compounds constitute a popular class of fluorescent molecules, and the well-established boron-dipyrromethene (BODIPY) series are a widely employed sub-class because of their excellent optical properties, including their high quantum yields and their strong stability to physiological conditions.[7] Another useful aspect of BODIPYs is that their emission wavelength can be systematically fine-tuned via minimal structural modifications.[8] However, despite the numerous achievements reached in this field, there is still a large interest in the discovery of new fluorophore families that offer short synthesis routes, facile structure modifications and good optical properties.[9]

During a program of research in our labs focused on cycloaddition approaches to benzene-[10] and heteroaromatic-boronic acid derivatives,[11] we uncovered a novel intramolecular cycloaddition paradigm that took advantage of the in situ formation of a Lewis acid-base complex (Scheme 1).[12] We were intrigued to find that products derived from this process exhibited strong fluorescence. Specifically, although many dyes contain the difluoroboryl group,[13] these are generally coordinated to two heteroatoms. Four-coordinate organoboron compounds based on *N,C* chelates are emerging as a useful sub-set of this family of fluorescent molecules,[14] although only a few reports on analogs possessing BF_2 group have been reported to-date.[15] As our cycloaddition chemistry offered the opportunity to assemble bespoke aromatic difluoroboranes, with the potential to vary substituents as a means of easily tailoring properties, we undertook an investigation of this novel class of fluorescent compounds, in order to better understand the scope and origin of their photophysical properties. We report herein the synthesis of a series of borylated bipyridines (BOBIPYs), their photophysical properties and the use of DFT calculations to account for the origin of their fluorescent behaviour.

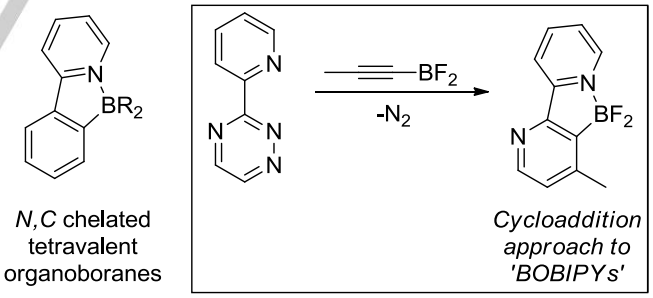

Scheme 1. Directed cycloaddition approach to fluorescent BOBIPYs.

Results and Discussion

Synthesis route to BOBIPYs: Our cycloaddition chemistry offered the opportunity to prepare benzene[16] and pyridine[12] substituted difluoroboranes, however, looking ahead to applications of our fluorescent molecules for cell imaging, we chose the latter compounds as the polar heterocycle core offered the prospect of increased water solubility versus a benzene derived analog. Moreover, in an effort to maximise our chances of obtaining a powerful fluorophore, we first set out to synthesise a target with an extended aromatic system. Accordingly, amidrazone **2a** was prepared from the

[a] S. P. J. T. Bachollet, Dr. J. Carillo, H. Adams, Prof. J. P. A. Harrity
Department of Chemistry
University of Sheffield
Brook Hill, Sheffield, S3 7HF (United Kingdom)
E-mail: j.harrity@sheffield.ac.uk
[b] S. P. J. T. Bachollet, S. Münch, Prof. S. Bräse
Institute of Organic Chemistry
Karlsruhe Institut of Technology
Fritz-Haber-Weg 6, D-76131 Karlsruhe (Germany)
E-mail: stefan.braese@kit.edu
[c] Dr. D. Volz
Cynora GmbH
Werner-von-Siemens-Straße 2-6, 76646 Bruchsal, (Germany)
[d] B. Fiser, E. Gómez-Bengoa
Departamento de Química Organica I
Universidad del País Vasco
Manuel Lardizabal 3, 20018 San Sebastian (Spain)
[e] F. Rönicke, Prof. U. Schepers
Institute of Toxicology and Genetics
Karlsruhe Institute of Technology
Hermann-von-Helmholtz-Platz 1, D-76344 Eggenstein-Leopoldshafen (Germany)

Supporting information for this article is available on the WWW under http://dx.doi.org/10.1002/chem.2014xxxxx.

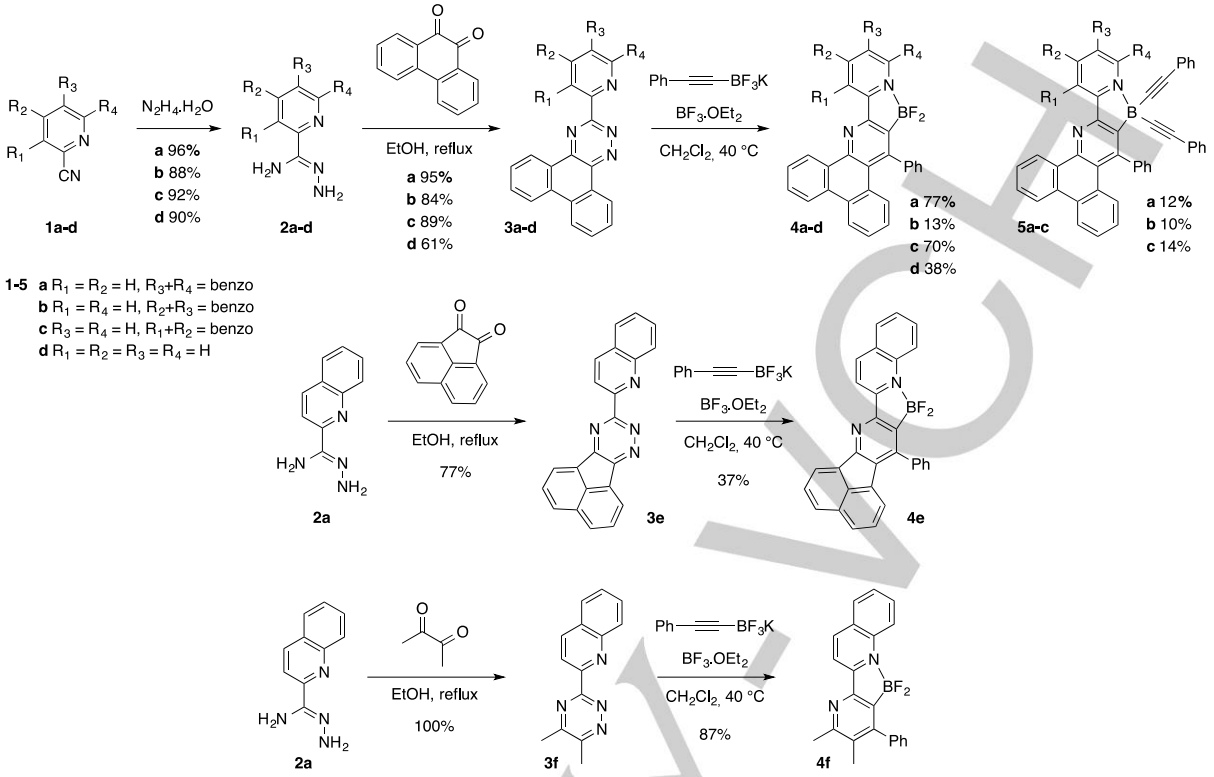

Scheme 2. Synthesis of BOBIPYs **4a-f** and **5a-c**.

corresponding nitrile and hydrazine, and condensation with 9,10-phenanthrenequinone afforded triazine **3a** (Scheme 2). Finally, cycloaddition with potassium phenylethynyltrifluoroborate afforded the first BOBIPY **4a** in good yield over the three steps. In order to investigate the influence of the conjugation pattern of the 3-borylated pyridine moiety, BOBIPYs **4e** and **4f** were also prepared in modest to good yields. In addition, the structure of the Lewis basic donor was varied and BOBIPYs containing isomeric isoquinoline donors **4b,c** and simple pyridyl analog **4d** were synthesized in acceptable overall yield. The directed cycloadditions are known to produce side-products bearing a dialkynylborane unit.[17] In this regard, three BOBIPYs **5a-c** were isolated that each contained alkynylboranes and we therefore decided to study the fluorescent properties of these compounds in order to establish the influence of the substituents at boron. Overall therefore, nine pyridyl boranes were generated within a simple reaction scheme that allowed rapid diversity at all key points in the fluorophore framework.

We were able to grow suitable quality crystals of compounds **4a**,**f** and **5a** for characterization by single-crystal X-ray diffraction (Figure 1).[18] The structures confirmed the four-coordinate boron center in each case, with the polycyclic core located in one plane within an extended aromatic system. Only the substituents at the boron and the phenyl ring originating from the alkyne are located out of the main plane of the molecules. The obtained structural information of **4f** has been used to validate the DFT-calculations and to interpret photo-physical properties.

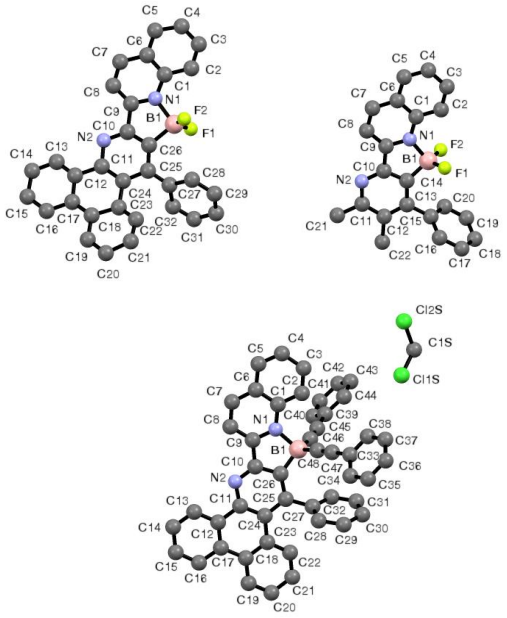

Figure 1. ORTEPs of BOBIPY **4a** (top left), **4f** (top right) and **5a** (bottom). Hydrogen atoms are omitted for clarity. Selected bond lengths [Å] and angles [°]: **4a**: N1-B1 1.728(2), C26-B1 1.719(2), F1-B1 1.345(2), F2-B1 1.310(1); N1-C9-C10-C26 -1.19(1), C8-C9-C10-N2 7.31(2); **4f**: N1-B1 1.657(3), C14-B1 1.620(3), F1-B1 1.384(2), F2-B1 1.387(3); N1-C9-C10-C14 -0.62(2), C8-C9-C10-N2 -1.28(3); **5a**: N1-B1 1.640(7), C26-B1 1.621(8), C46-B1 1.591(9), C48-B1 1.577(1); N1-C9-C10-C26 -1.21(7), C8-C9-C10-N2 -4.90(9).

Table 1. Basic spectroscopic data of fluorophores **4a-f** and **5a-c** in dichloromethane.

Compound	λ_{abs} (nm)	ε ($M^{-1}.cm^{-1}$)	λ_{em} (nm)	Stokes shift (nm)	PLQY Φ
4a	388	22921	473	85	0.33
4b	377	20497	452	75	0.08
4c	392	13358	467	75	0.23
4d	373	17901	424	51	0.12
4e	421	40587	465	44	0.41
4f	376	15396	423	47	0.13
5a	400	25245	456	56	0.13
5b	381	29729	420	39	0.11
5c	408	17218	453	45	0.11

*Photophysical Properties of BOBIPYs **4a-f, 5a-c**:* The photophysical properties of all new fluorophores are summarized in Table 1 and Table 2.[19] We note that excitation spectra were measured by monitoring the peak emission of the respective compounds and that emission spectra were obtained by excitation at 365 nm for each sample. Owing to the high diversity of the structures synthesized herein, the emission color in dichloromethane solution varied between 420 and 473 nm, the absorption spectra are significantly different for each substitution pattern and both Stokes shifts and photoluminescent quantum yield (PLQY) cover a broad range. The emission spectra were broad and ill-structured.

Table 2 contains the excited state decay time τ for **4a-f** and **5a-c**. If there are no quenching factors (impurities, trace amounts of solvent) present,[20] the PLQY Φ can be generally formulated as a function of the decay lifetime τ as $\Phi = k_r\tau$, with k_r: radiative decay rate. Additionally, with the relation: $\tau^{-1} = k_r + k_{nr}$, the non-radiative decay rate k_{nr} can be calculated. This set of equations is valid for a mono-exponential emission decay, e.g. for fluorescence of organic molecules.[21] According to the rule of Kasha and Vavilov,[22] Φ is independent of the observed wavelength in those cases and the same applies for k_r and τ. Based on these assumptions, we calculated values for k_r and k_{nr}, which are given in Table 2.

The relative error on τ is usually in the order of 25%, while the Φ can be determined with an absolute error of ±0.02. In the worst case (**4b**) this means an additional relative error of 25%. Due to propagation of this uncertainty, the relative error of k_r is 35%. For k_{nr}, the relative error is roughly the same. With this, it is possible to draw qualitative conclusions based on this data.

As indicated in Table 2, the new BOBIPYs show promising properties with PLQY values up to 41% and an emission color from blue to green with ideal Stokes shifts. The different trends, which can be related to the molecular structure, will be discussed below. Additionally, BOBIPYs also show solid state luminescence. This has been established for samples **4a**, **4d** and **4e**. The emission spectra as well as the PLQY values differ from solution measurements, as expected: **4a**, **4d** and **4e** emit in solid state at 490 nm, 450 nm and 504 nm, respectively, with PLQY values of 0.24, 0.20 and 0.19. The overlap between absorption and emission spectra in solution suggests that complex, intermolecular energy transfer processes occur in solid state, where the chromophores are close to each other.

Table 2. Excited state lifetime and estimation of radiative and non-radiative decay constants k_r and k_{nr} in dichloromethane.

Compound	τ [ns]	Φ	k_r [10^8 s^{-1}]	k_{nr} [10^8 s^{-1}]
4a	2.6	0.33	1.2	2.6
4b	2.0	0.08	0.4	1.0
4c	1.8	0.23	1.3	4.3
4d	1.6	0.12	0.8	5.5
4e	3.7	0.41	1.1	1.6
4f	2.1	0.13	0.6	4.2
5a	1.4	0.13	0.9	6.2
5b	7.1	0.11	0.2	1.2
5c	1.4	0.11	0.8	6.3

DFT calculations. Overview of structural and electronic properties: In order to gain an insight into the origin of the fluorescence and the effects that cause the surprising and significant difference between the optical properties of these closely related compounds, DFT calculations were carried out. Fluorophores **4a-f** and **5a-c**, together with a BF_2-containing BODIPY analog **6** (Figure 2), were optimized using the B3LYP functional[23] combined with the 6-31G(d) basis set[24] as implemented in Gaussian 09 program package.[25] The level of theory B3LYP/6-31G(d) was selected based on the fact that it was previously successfully applied to calculate similar systems.[26]

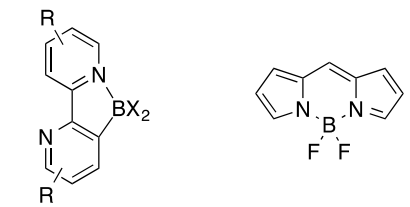

BOBIPY **4a-f**, **5a-c** BODIPY **6**

Figure 2. General structure of BOBIPYs (**4a-f**, **5a-c**) and BODIPY **6** used for comparison of optical properties.

Table 3. LUMO and HOMO energies with the corresponding energy gaps calculated in gas phase, dichloromethane (DCM) and water.

	HOMO /eV			LUMO /eV			Gap /eV		
	Gas	**DCM**	**Water**	**Gas**	**DCM**	**Water**	**Gas**	**DCM**	**Water**
4a	-5.77	-5.99	-6.02	-2.50	-2.56	-2.58	3.27	3.43	3.44
4b	-5.68	-5.89	-5.92	-2.32	-2.24	-2.24	3.36	3.65	3.68
4c	-5.79	-5.97	-5.99	-2.50	-2.56	-2.57	3.29	3.41	3.42
4d	-5.80	-5.99	-6.02	-2.19	-2.23	-2.24	3.61	3.76	3.78
4e	-5.85	-6.05	-6.08	-2.46	-2.58	-2.60	3.39	3.47	3.48
4f	-6.20	-6.34	-6.36	-2.35	-2.43	-2.44	3.85	3.91	3.92
5a	-5.51	-5.91	-5.96	-2.45	-2.53	-2.55	3.06	3.38	3.41
5b	-5.54	-5.84	-5.89	-2.28	-2.23	-2.22	3.26	3.61	3.67
5c	-5.47	-5.89	-5.93	-2.44	-2.50	-2.52	3.03	3.39	3.41

Furthermore, TD-DFT calculations were carried out at the same level of theory. Solvent effects of dichloromethane and water were taken into account for the optimizations at the same level of theory by applying the conductor-like polarizable continuum model. The intramolecular reorganization energies (λ_{hole} and $\lambda_{electron}$) of the studied compounds were also computedThe acquired X-ray structure of compound **4f** (c.f. Figure 1) was compared to its gas phase optimized counterpart to verify the selected level of theory from a structural point of view. Root-mean-square deviation (RMSD) was calculated to measure the difference between the experimental and calculated geometries. Pleasingly, the RMSD value was found to be rather small (0.224 Å) proving confidence that the applied level of theory was appropriate.[27]

Molecular orbital plots and orbital energies for BOBIPYs **4a-f**, **5a-c** and BODIPY **6** were calculated and the results are summarized in Table 3 and molecular orbital plots of selected structures presented in Figure 3.[28] The HOMO to LUMO excitation is dominant in most of the BOBIPYs, in a similar manner to BODIPY **6**. There are two other excitations (HOMO-2 to LUMO and HOMO to LUMO+1), which are also important in some cases, and this issue will be discussed later. The HOMO and LUMO orbital energies of gas and solvent phase calculations were compared and, in most cases, the energies decreased when solvents were incorporated (Table 3).[28]

The orbital localization is very similar in both phases for BODIPY **6** and **4a-f**, but not for **5a-c** (Figure 3).[28] Specifically, **5a-c** are the biggest systems within the studied set of molecules because of the two phenylacetylene groups substituting the boron. The deviations between the orbital localizations arise from the fact that the rotation of these groups lead to different minima in different phases, which changes the localization of the HOMOs. Nevertheless, the solvent phase results are consistent and match the experimental conditions. For these reasons, the following discussion will be focused on the results obtained in dichloromethane.

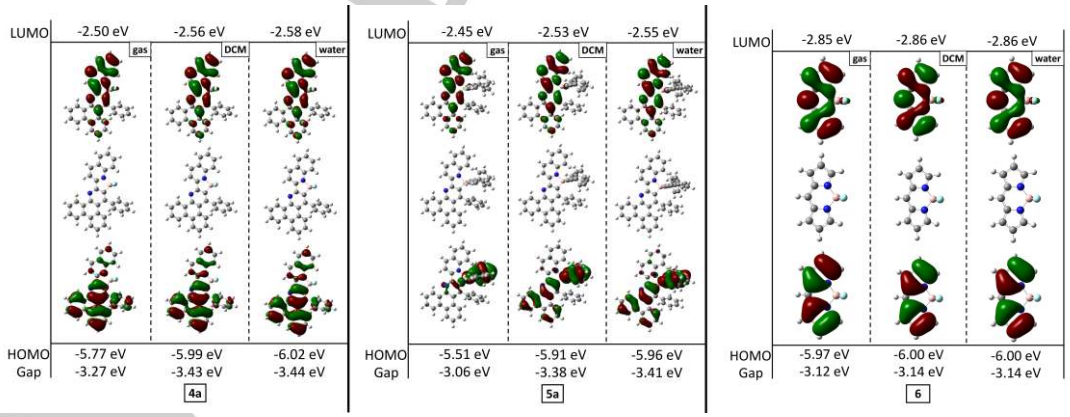

Figure 3. Molecular orbital plots and orbital energies of **4a**, **5a** and BODIPY **6** along their optimized structures (middle row) in gas phase and in solvents.

Structure-photophysics relationship: The impact of the molecular structure of the BOBIPYs on the photophysical properties was next investigated. For convenience, we will discuss structure-property relationships for three variables (Figure 4), and have designated these the northern ring (I), the borane (II) and the southern ring (III). As highlighted earlier, the synthetic approach employed provided a modular method for the structural modification of both the northern and southern rings, while the substitution of the boron group results from the cycloaddition step.

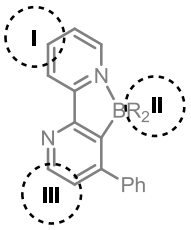

Figure 4. Three easily modifiable positions in the general skeleton of the BOBIPYs.

Variation of the northern ring (I) and borane (II) on photophysics properties: The impact of the substitution pattern of the northern ring on photophysical properties was assessed by comparing compounds **4a-d** and **5a-c**. Moreover, the effect of varying the nature of the borane could be observed by comparing each pair **4a**/**5a** to **4c**/**5c**, where the substitution pattern around the boron atoms is changed from B-F to B-(phenylacetylide) (Figure 5). Figures 5a and 5b show the absorption and emission spectra for these seven compounds.

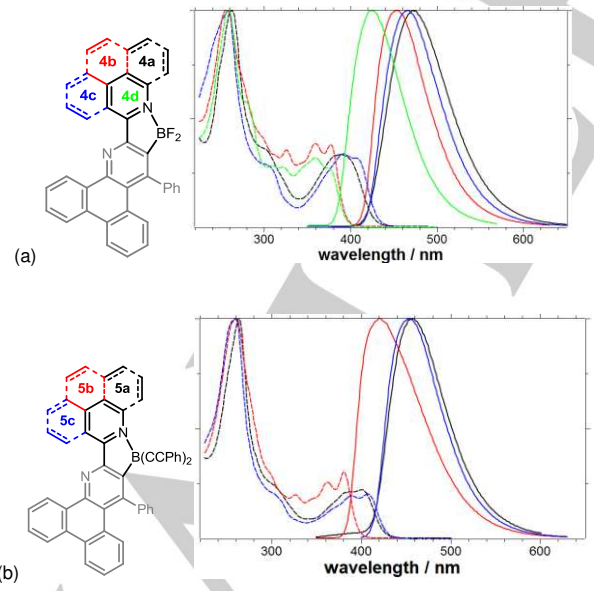

Figure 5. Normalized absorption (left) and emission spectra (right) of compounds **4a-d** (a) and **5a-c** (b) in CH_2Cl_2. The color of the ring systems indicates the color of the respective spectra in (a) and (b).

The qualitative shape of the spectra is dominated by the ring systems: **4b, 4d** and **5b** differ from the other compounds. Their PLQY is considerably lower and the absorption spectra are more structured and the low-energy bands associated with the HOMO-LUMO transition are blue-shifted compared to **4a**/**4c** and **5a**/**5c**, while the π-π* transitions around 260 nm are not. The emission spectra are also blue shifted, suggesting that the bandgap of **4b, 4d** and **5b** is larger. Analysis of the excited state lifetime reveals interesting trends: both radiative rates k_r and non-radiative rates k_{nr} are considerably lower. The low k_r values over-compensate the k_{nr} values, yielding a very low overall PLQY.

The substituents attached at boron do not seem to affect the absorption spectra too much – the spectra are almost superimposable, which shows that photoexcitation initially leads to similar excited states. This suggests that neither the HOMO, nor the LUMO are localized on the BR_2 units. On the other hand, the emission spectra are significantly different. **4a**/**5a** and **4c**/**5c** have similar energies, while **4b**/**5b** are slightly higher, showing that the main trends seem to be dictated by the relative orientation of the quinoline/isoquinoline rings. For the BF_2-compounds, the emission is red shifted, the PLQY is much higher and the Stokes shifts are larger. Analysis of k_r and k_{nr} reveals that the radiative processes are similar, while non-radiative processes seem to be more dominant, yielding an overall decrease of the PLQY. This suggests that the B-substituents affect the excited molecules, either by opening up addition quenching pathways (e.g. by vibronic quenching) or by steric or electronic effects.

In all seven cases, several transitions of similar energy and relative extinction are present in the absorption spectra, even though they are poorly resolved for **4a**/**4c** and **5a**/**5c**. The emission spectra show one broad, ill-structured emission in each case, while the Stokes shifts are fairly large. This indicates a certain charge-transfer character of the emissive transition.
Analysis of the photophysical properties of **4a-d** and **5a-c** suggests that either the HOMO or the LUMO is likely to be localized on the quinoline/isoquinoline moiety, while the BR_2 units seems to have an indirect effect on the photophysical properties, caused by steric or electronic effects. A strong charge-transfer character is likely.

DFT analysis of variation of the northern ring (I) and borane (II): In general, the LUMO is mainly localized on the heterocycle next to the BF_2 moiety, whereas the HOMO spreads over almost the whole molecule with the exception of the borane moiety (Figure 3).[28] The phenyl group does not contribute to the LUMO and slightly contributes to the HOMO of these molecules, probably because its out of the plane conformation offers less electronic coupling. The LUMO energies are the same for **4a** and **4c** (-2.56 eV, in DCM), while there is a small difference between their HOMO energies (0.02 eV). Thus, the HOMO-LUMO gaps are also very close to each other (3.43 and 3.41 eV, for **4a** and **4c**, respectively). The calculated maximum absorption wavelength of **4a** and **4c** are also close (416.3 and 418.7 nm) and both of them assigned to the $S_0 \rightarrow S_1$ electronic transition with an excitation energy of 2.98 and 2.96 eV, respectively.[28]

Compared to **4a** or **4c**, **4b** has higher LUMO (-2.24 eV) and HOMO (-5.89 eV) energies and its energy gap is also wider (3.65 eV). This is in good agreement with the fact that its measured emission wavelength is smaller**.** The phenanthrene moiety does not contribute to the LUMO of **4b**, which could be one of the reasons why this compound has a lower quantum yield than its isomers (**4a** and **4c**). The calculated λ_{abs} (371.7 nm) of **4b** with the strongest oscillator strength is in very good agreement with the measured value (377.0 nm). Its excitation wavelength is assigned to the $S_0 \rightarrow S_2$ electronic transition from HOMO to LUMO+1 where the excitation energy is 3.34 eV.[28]

The measured emission wavelength of **4d** is even smaller than **4b**, which is in agreement with its bigger HOMO-LUMO gap (3.76 eV). The measured and calculated absorption maxima are very close to each other ($\Delta\lambda$ = 4 nm) and assigned to the $S_0 \rightarrow S_1$ transition, but the excitation energy is higher by around 0.3 eV. Despite the contribution of the phenanthrene moiety of **4d** to its LUMO, the measured quantum yield is smaller (0.12) than in the case of **4a-c**, probably because of the decreased area of delocalization when changing from a (iso)quinoline to a pyridine as directing group. Finally, the calculated λ_{abs} values of **5a-c** are in good agreement with the measured ones. In these cases, the electronic transition with the strongest oscillator strength is $S_0 \rightarrow S_3$ from HOMO-2 to LUMO and HOMO to LUMO+1 for **5a**/**5c** and **5b**, respectively.[28]

Overall therefore, these findings are in agreement with the photophysical measurements, as they show that the phenylacetylene substituents affect the photophysical properties of the molecules (different electronic transitions), but the position of the quinoline/isoquinoline rings is more crucial.

Variation of the southern ring (III) on photophysics properties: In order to examine the effect of the southern ring on photophysical properties, we recorded absorption and emission spectra for compounds **4a**, **4e** and **4f**. The spectra are shown in Figure 6, PLQY and lifetime data is collected in Table 1 and Table 2.

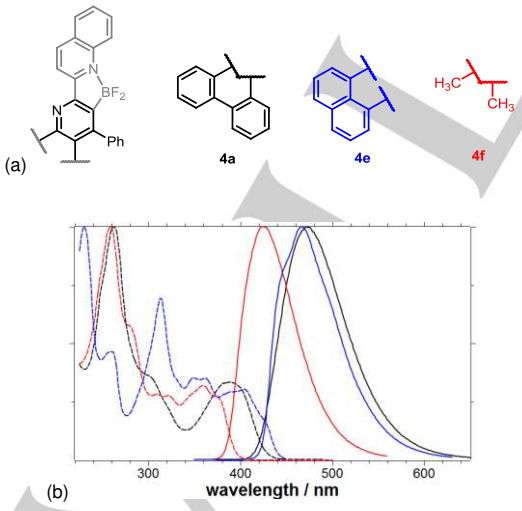

Figure 6. Normalized absorption (left) and emission spectra (right) of compounds **4a**, **4e** and **4f** in CH_2Cl_2. The color of the depicted subunits in (a) indicates the color of the respective spectra in (b).

Both emission and absorption spectra in Figure 6 are essentially unique to each compound, indicating that modification of (III) has a strong impact on the frontier orbitals and the electronic states. For **4f**, a rather localized π-system is present, which yields relatively high emission energy in both absorption and emission spectra. Although the PLQY is rather low (11%, Table 1). A comparison of the k_r and k_{nr} values of **4f** and **4a** shows significant differences for both radiative and non-radiative processes. This, together with the strong qualitative difference in the absorption spectra, suggests that the electronic state of these two systems differ greatly. For **4e**, both emission and absorption spectra differ greatly from the other compounds analyzed in this study: besides the fact that the emission shows a slightly structured profile, the absorption spectra shows an additional high energy band around 230 nm. Also, the relative extinction coefficient of the low energy bands around 420 nm is almost a factor of two higher than for all other compounds in the study (see Table 1). These results point towards a more localized transition for this compound, especially compared to reference compound **4a**. In summary, variation of position III allows for an even stronger manipulation of the optoelectronic properties than positions I and II.

DFT analysis of variation of the southern ring (III): The HOMO of **4f** is less delocalised because of its structure, which lowers its energy and thus results in the largest HOMO-LUMO gap (3.91 eV) within the whole set of BOBIPYs. The highest quantum yield (0.41) was found in the case of **4e** and it also has the lowest reorganization energy for electron transfer ($\lambda_{electron}$ = 0.24 eV).[28] In **4e** the whole structure (except the phenyl group) is arranged in one plane and this helps the delocalization, while in **4a** there is a slight twist between the isoquinoline and the phenanthrene moiety (Figure 7), which results in a less electronically coupled system and a smaller quantum yield than in **4e**.

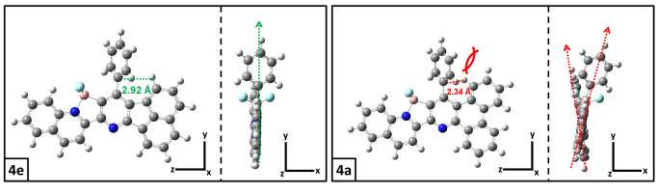

Figure 7. Structural differences between the optimized **4e** and **4a** in dichloromethane.

Stability studies: To assess the potential of our new BOBIPY series for biological applications, we next studied its stability under different conditions, using **4f** as reference. Similar structures have been shown to be stable to nucleophilic substitution processes, photochemical reactions, temperature variations and in buffered solutions.[14b] We thus focused on the stability of the fluoroborane group as this had not been previously established. Submission to mild nucleophilic conditions that could be encountered during applications (namely, $NaOH_{(aq)}$ in THF at room temperature) returned the fluorophore untouched, confirming the hydrolytic stability of the

BF_2 moiety under these conditions. In contrast however, subjecting **4f** to base in refluxing THF returned the corresponding boronic acid **7** in high yield (Scheme 3). Upon crystallization in ethanol, we were able to obtain **8**, which was characterized by X-ray crystallography (Figure 8).

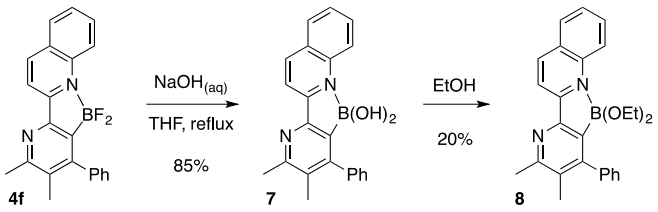

Scheme 3. Synthesis of **7** and **8**.

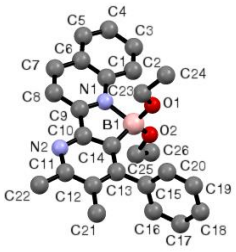

Figure 8. ORTEP of BOBIPY **8**. Hydrogen atoms are omitted for clarity. Selected bond lengths [Å] and angles [°]: N1-B1 1.762(2), C14-B1 1.628(3), O1-B1 1.425(3), O2-B1 1.420(2); N1-C9-C10-C14 2.95(2), C8-C9-C10-N2 2.64(3).

Interestingly, changing the boron-substituents from F to OH or OEt has a much greater impact on the optical properties of these compounds than the change from F to arylacetylide. In contrast to **4f** and **5a-c**, both **7** and **8** exhibit quantum yield values lower than our limits of detection. We also compared the absorption spectra for **4f**, **7** and **8**.[28] Not surprisingly, spectra for **7** and **8** are almost superimposable. While no significant changes apart from slight broadening was observed for **4a-c** versus **5a-c,** the low-energy band is blue-shifted for **7**/**8**, as are other features, which indicates that the electronic states are affected by the introduction of the oxygen-substituents. The X-ray structures of **4f** and **8** were also used as model structures for DFT calculations and were studied computationally together with **7**. The corresponding B-X distances were collected and compared. The boron-carbon distances are similar in each case, while the B-N distances are longer by ~0.1 Å in **7** and **8**.[28] HOMO and LUMO molecular orbital plots of **4f, 7** and **8** were also compared. The localization of the orbitals is very similar in each case, but the orbital energies are changed as the substituents are changed from F to OH or OEt.[28] The orbital energies of **7** and **8** calculated in DCM are shifted towards higher values by 0.15 and 0.12 eV for HOMO and by 0.28 and 0.22 eV for LUMO orbitals in the case of **7** and **8**, respectively. The HOMO-LUMO gaps are also increased by 0.13/0.1 eV for **7**/**8** and surpass 4 eV. Pais and co-workers have studied related systems with isoquinoline, aryl-substituents and boronic ester groups, and highlighted that planarization of the biaryl system can have an adverse impact on fluorescence efficiency.[14c] In this case, the authors presented hints for a temperature-dependent ring-opening of the B-heterocycle. A similar process could in principle take place in our case, since the analogous twisted conformation exists for **7**. However, we believe that this is unlikely in practice as the energy difference is quite high (ΔG=5.7 kcal/mol), favoring the structure in which B-N coordination is preserved. The underlying structure-property relationships appear rather complex as boronic esters in this class can show fluorescence with highly variable quantum yields.[29]

Tuning BOBIPYs for bioapplications: We believed that compound **4a** showed the best overall combination of useful photophysical properties and chemical accessability, making it the most suitable BOBIPY to exploit for cell uptake and imaging studies. The quantum efficiency of **4a** in solution is in the order of 35% and the emission color is in the green region of the optical spectrum. The broad absorption band, which is well above 400 nm should allow for excitation with blue light rather than UV light sources, which is mandatory to perform fluorescence microscopy experiments without risking photo-damage. Also, a rather high Stokes shift allows for good distinction of the emitted light from the excitation light, as well as distinction of the fluorophore from auto-fluorescence of biological tissue.

As indicated by the DFT calculations, further tuning of the color seems feasible to allow for creation of yellow or red-emitting compounds. This is best done by addition of electron-donating groups to the southern heterocycle unit (III) of the molecule, where the HOMO is localized, and/or addition of electron-withdrawing groups to the northern ring (I), where the LUMO is localized (Figure 9). With this, the optical bandgap could be decreased. The phenyl ring attached to **4a** is not a significant part of either HOMO or LUMO, and can be used to add further functionality (Figure 9), e.g. solubilizing groups or transporters, which can be used to facilitate uptake in living cells.

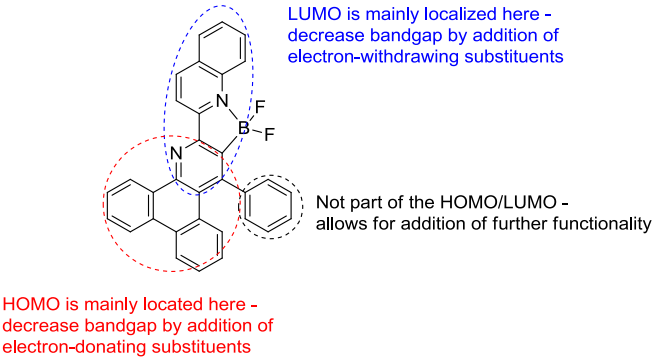

Figure 9. Modification of the fluorophore **4a** allows for further color-tuning or the addition of more functionalities.

As a proof-of-principle, we designed a BOBIPY bearing a free alkyne function that would offer the opportunity to be covalently attached to any substrate of interest by means of a 'click' reaction. Alkyne **9** was thus prepared and its cycloaddition with triazine **3a** afforded fluorophore **4g**, equipped with a free alkyne (Scheme 4).

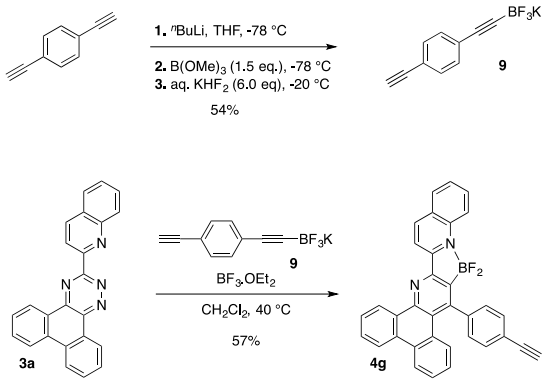

Scheme 4. Synthesis of **4g**.

The properties of **4a** and **4g** are very similar to each other, which was expected, because the difference between their structure is located on the electronically less coupled phenyl group. The difference between their HOMO-LUMO gap is only 0.02 eV, while their emission wavelengths are identical (473 nm). The absorption and emission spectra of the two compounds **4a** and **4g** are almost superimposable,[28] while the high PLQY is maintained even after addition of the conjugated alkyne group (Table 4). Importantly, for other emissive compounds, the addition of conjugated groups can lead to significant differences.[30]

Table 4. Photophysical properties of **4g** compared to **4a** in dichloromethane.

Compound	**4a**	**4g**
λ_{abs} (nm)	388	389
ε ($M^{-1}.cm^{-1}$)	22921	22252
λ_{em} (nm)	473	473
Stokes shift (nm)	85	84
PLQY Φ	0.33	0.31
τ [ns]	2.6	2.4
k_r [10^8 s^{-1}]	1.2	1.3
k_{nr} [10^8 s^{-1}]	2.6	2.9

To demonstrate the suitability of **4g** to track molecules *in vivo*, we coupled it to a peptoid bearing an azide side chain on solid phase in a sub-monomer approach using copper iodide and *N,N*-diisopropylethylamine (DIPEA). This peptoid is a hexameric compound with five aminobutyl- and one azidopropyl-side chain and was designed to enhance the water-solubility of the final compound (Scheme 5). Peptoid **10** was characterized in aqueous solution.[28] The insolubility of **10** in organic solvents, coupled with to the insolubility of **4a** and **4g** in water, prevented any direct comparison of the impact of solvent polarity on their photophysical properties. Measurements revealed that **10** emits around 510 nm in water, in the green region, and maintains high PLQY values. The red shift compared to the DCM-measurements of **4a** and **4g** is likely to be a result of a more polar environment, which affects the emission by stabilization of the charge transfer transitions.

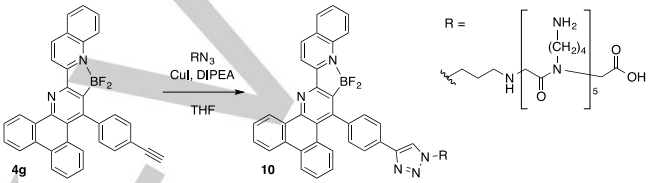

Scheme 5. Synthesis of peptoid **10**.

To examine the cell compatibly, human cervix carcinoma (HeLa) cells were treated with peptoid **10** for 24 hours and subsequently imaged with a confocal fluorescence microscope. The results confirmed the accumulation of the compound in endosomal vesicles, indicating an endocytotic uptake (Figure 10). With this method, the intracellular location of **10** could be detected and this demonstrates the potential of BOBIPYs for biological imaging.

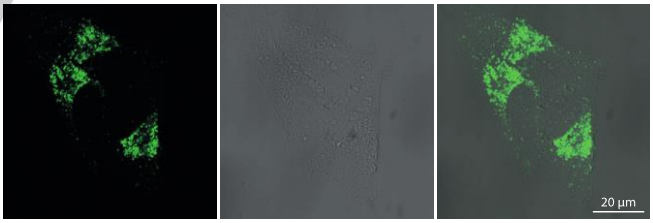

Figure 10. Fluorescent confocal microscopy of **10** in HeLa cells. Left: Emission at 458 nm, Excitation: at 458 nm; Middle: Brightfield; Right: Merge. For further conditions see SI.

Conclusions

In conclusion, we have developed a new strategy for the design, synthesis and optical tuning of a family of borylated bipyridines (BOBIPYs). The photophysical properties of these compounds have been measured, and the results interrogated by DFT calculations. With respect to the tetravalent N,C-linked boron atom of these BOBIPYs, the LUMO is located on the C,N-linking bipyridine-type group, while the HOMO is located mainly in the

C-linking aryl moiety. The modular synthesis of BOBIPYs offers a simple way to tune optical properties, while substituents incorporated from the key cycloaddition step of alkynyl trifluoroborates provide an effective means for the incorporation of these compounds onto various molecular scaffolds. Indeed, we have exemplified the potential applicability of BOBIPYs for cellular imaging by carrying out conjugation to a peptoid and imaging the compound within human cervix carcinoma cells.

Experimental Section

The procedures for the synthesis, optical properties, theoretical calculations and applications for biological imaging are provided in the Supporting Information.

Acknowledgements

This work was supported by the FP7 Marie Curie Actions of the European Commission via the ITN ECHONET Network (MCITN-2012-316379), GRK 2039 and the BioInterfaces International Graduate School.

Keywords: fluorophore • borylated bipyridines • density functional calculations • cell imaging • photophysics

[1] Friend, R. H.; Gymer, R. W.; Holmes, A. B.; Burroughes, J. H.; Marks, R. N.; Taliani, C.; Bradley, D. D. C.; Santos, D. A. D.; Brédas, J. L.; Lögdlund, M.; Salaneck, W. R. *Nature* **1999**, *397*, 121-128.

[2] Benstead, M.; Mehl, G. H.; Boyle, R. W. *Tetrahedron* **2011**, *67*, 3573-3601.

[3] Hörner, A.; Volz, D.; Hagendorn, T.; Fürniss, D.; Greb, L.; Rönicke, F.; Nieger, M.; Schepers, U.; Bräse, S. *RSC Adv.* **2014**, *4*, 11528-11534.

[4] Boens, N.; Leen, V.; Dehaen, W. *Chem. Soc. Rev.* **2012**, *41*, 1130-1172.

[5] (a) Kamkaew, A.; Lim, S. H.; Lee, H. B.; Kiew, L. V.; Chung, L. Y.; Burgess, K. *Chem. Soc. Rev.* **2013**, *42*, 77-88; (b) Gibbs, J. H.; Zhou, Z.; Kessel, D.; Fronczek, F. R.; Pakhomova, S.; Vicente, M. G. H. *J. Photochem. Photobiol., B* **2015**, *145*, 35-47.

[6] Haugland, R. P. *Handbook of Fluorescent Probes and Research Chemicals*, 6th ed.; Molecular Probes: Eugene, OR, 1996.

[7] Loudet, A.; Burgess, K. *Chem. Rev.* **2007**, *107*, 4891-4932.

[8] Santra, M.; Moon, H.; Park, M.-H.; Lee, T.-W.; Kim, Y. K.; Ahn, K. H. *Chem. Eur. J.* **2012**, *18*, 9886-9893.

[9] (a) Li, Z.; Lv, X.; Chen, Y.; Fu, W.-F. *Dyes and Pigments* **2014**, *105*, 157-162; (b) Wu, Y.; Li, Z.; Liu, Q.; Wang, X.; Yan, H.; Gong, S.; Liu, Z.; He, W. *Org. Biomol. Chem.* **2015**, *13*, 5775-5782; (c) Zimmerman, J. R.; Johntony, O.; Steigerwald, D.; Criss, C.; Myers, B. J.; Kinder, D. H. *Org. Lett.* **2015**, *17*, 3256-3259.

[10] (a) Stalling, T.; Harker, W. R. R.; Auvinet, A.-L.; Cornel, E. J.; Harrity, J. P. A. *Chem. Eur. J.* **2015**, *21*, 2701-2704; (b) Auvinet, A.-L.; Harrity, J. P. A.; Hilt, G. *J. Org. Chem.* **2010**, *75*, 3893-3896; (c) Delaney, P. M.; Browne, D. L.; Adams, H.; Plant, A.; Harrity, J. P. A. *Tetrahedron* **2008**, *64*, 866-873.

[11] (a) Comas-Barceló, J.; Foster, R. S.; Fiser, B.; Gomez-Bengoa, E.; Harrity, J. P. A. *Chem. Eur. J.* **2015**, *21*, 3257-3263; (b) Huang, J.; Macdonald, S. J. F.; Harrity, J. P. A. *Chem. Commun.* **2009**, *45*, 436-438.

[12] Bachollet, S. P. J. T.; Vivat, J. F.; Cocker, D. C.; Adams, H.; Harrity, J. P. A. *Chem. Eur. J.* **2014**, *20*, 12889-12893.

[13] Frath, D.; Massue, J.; Ulrich, G.; Ziessel, R. *Angew. Chem. Int. Ed.* **2014**, *53*, 2290-2310.

[14] (a) Shaikh, A. C.; Ranade, D. S.; Thorat, S.; Maity, A.; Kulkarni, P. P.; Gonnade, R. G.; Munshi, P.; Patil, N. T. *Chem. Commun.* **2015**, *51*, 16115-16118; (b) Pais, V. F.; Alcaide, M. M.; López-Rodríguez, R.; Collado, D.; Nájera, F.; Pérez-Inestrosa, E.; E., Á.; Lassaletta, J. M.; Fernández, R.; Ros, A.; Pischel, U. *Chem. Eur. J.* **2015**, *21*, 15369-15376; (c) Pais, V. F.; Lassaletta, J. M.; ndez, R. F.; El-Sheshtawy, H. S.; Ros, A.; Pischel, U. *Chem. Eur. J.* **2014**, *20*, 7638-7645; (d) Rao, Y.-L.; Wang, S. *Inorg. Chem.* **2011**, *50*, 12263-12274; (e) Yusuf, M.; Liu, K.; Guo, F.; Lalancette, R. A.; Jäkle, F. *Dalton Trans* **2016**, *45*, 4580-4587.

[15] (a) Frizler, M.; Yampolsky, I. V.; Baranov, M. S.; Stirnberg, M.; Gütschow, M. *Org. Biomol. Chem.* **2013**, *11*, 5913-5921; (b) Baranov, M. S.; Solntsev, K. M.; Baleeva, N. S.; Mishin, A. S.; Lukyanov, S. A.; Lukyanov, K. A.; Yampolsky, I. V. *Chem. Eur. J.* **2014**, *20*, 13234 – 13241.

[16] Kirkham, J. D.; Butlin, R. J.; Harrity, J. P. A. *Angew. Chem. Int. Ed.* **2012**, *124*, 6508-6511.

[17] Crépin, D. F. P.; Harrity, J. P. A.; Jiang, J.; Meijer, A. J. H. M.; Nassoy, A.-C. M. A.; Raubo, P. *J. Am. Chem. Soc.* **2014**, *136*, 8642-8653.

[18] The supplementary crystallographic data for compounds 4a, 4f, 5a and 8 have been deposited with the Cambridge Crystallographic Data centre as supplementary publication numbers CCDC 1451469-1451472, respectively. These data can be obtained free of charge from the Cambridge Crystallographic Data centre via http://www.ccdc.cam.ac.uk/data_request/cif.

[19] Full spectra of all compounds are contained in the supporting information.

[20] Lakowicz, J. R. *Principles of Fluorescence Spectroscopy*, 3rd ed.; Springer: New York, 2006.

[21] O'Connor, D. V.; Ware, W. R.; Andre, J. C. *J. Phys. Chem.* **1979**, *83*, 1333-1343.

[22] IUPAC. Compendium of Chemical Terminology, 2nd ed. (the "Gold Book"). Compiled by A. D. McNaught and A. Wilkinson. Blackwell Scientific Publications, Oxford (1997).

[23] Becke, A. D. J. *J. Chem. Phys.* **1993**, *98*, 1372-1377.

[24] Petersson, G. A.; Bennett, A.; Tensfeldt, T. G.; Al-Laham, M. A.; Shirley, W. A.; Mantzaris, J. *J. Chem. Phys.* **1988**, *89*, 2193-2218.

[25] Frisch, M. J.; Trucks, G. W.; Schlegel, H. B.; Scuseria, G. E.; Robb, M. A.; Cheeseman, J. R.; Scalmani, G.; Barone, V.; Mennucci, B.; Petersson, G. A.; Nakatsuji, H.; Caricato, M.; Li, X.; Hratchian, H. P.; Izmaylov, A. F.; Bloino, J.; Zheng, G.; Sonnenberg, J. L.; Hada, M.; Ehara, M.; Toyota, K.; Fukuda, R.; Hasegawa, J.; Ishida, M.; Nakajima, T.; Honda, Y.; Kitao, O.; Nakai, H.; Vreven, T.; Montgomery, J. A., Jr.; Peralta, J. E.; Ogliaro, F.; Bearpark, M.; Heyd, J. J.; Brothers, E.; Kudin, K. N.; Staroverov, V. N.; Kobayashi, R.; Normand, J.; Raghavachari, K.; Rendell, A.; Burant, J. C.; Iyengar, S. S.; Tomasi, J.; Cossi, M.; Rega, N.; Millam, J. M.; Klene, M.; Knox, J. E.; Cross, J. B.; Bakken, V.; Adamo, C.; Jaramillo, J.; Gomperts, R.; Stratmann, R. E.; Yazyev, O.; Austin, A. J.; Cammi, R.; Pomelli, C.; Ochterski, J. W.; Martin, R. L.; Morokuma, K.; Zakrzewski, V. G.; Voth, G. A.; Salvador, P.; Dannenberg, J. J.; Dapprich, S.; Daniels, A. D.; Farkas, O.; Foresman, J. B.; Ortiz, J. V.; Cioslowski, J.; Fox, D. J. *Gaussian 09*, Revision B.1; Gaussian, Inc.: Wallingford, CT, 2009.

[26] Yuan, L.; Lin, W.; Yang, Y.; Chen, H. *J. Am. Chem. Soc.* **2012**, *134*, 1200-1211.

[27] For more details on the comparison of calculated and measured structural properties and on calculations of molecular orbital plots and maximum absorption wavelengths, see Supporting Information.

[28] The complete list of molecular orbital plots; absorption spectra obtained by TD-DFT calculations; calculated reorganisation energies; compared absorption spectra and calculated and measured B-X bond lengths; can be found in the Supporting Information.

[29] Pais, V. F.; El-Sheshtawy, H. S.; Fernández, R.; Lassaletta, J. M.; Ros, A.; Pischel, U. *Chem. Eur. J.* **2013**, *19*, 6650-6661.

[30] Volz, D.; Nieger, M.; Friedrichs, J.; Baumann, T.; Bräse, S. *Inorg. Chem. Commun.* **2013**, *37*, 106-109.

Entry for the Table of Contents

FULL PAPER

Lighting the way: a family of borylated bipyridines (BOBIPYs) fluorophores offers tunable optical properties and linker possibilities via a designed strategy of synthesis. The photophysical properties of these compounds have been measured, and the results interrogated by DFT calculations, enabling the mapping of the structure for further implementations.

$\lambda_{emission}$ = 420-475 nm
$\lambda_{excitation}$ = 380-410 nm
up to 0.41

Sylvestre P. J. T. Bachollet, Daniel Volz, Béla Fiser, Stephan Münch, Franziska Rönicke, Jokin Carrillo, Harry Adams, Ute Schepers, Enrique Gómez-Bengoa, Stefan Bräse and Joseph P. A. Harrity**

Page No. – Page No.

A Modular Class of Fluorescent Difluoroboranes: Synthesis, Structure, Optical Properties, Theoretical Calculations and Applications for Biological Imaging